
CHALMERS
UNIVERSITY OF TECHNOLOGY

# Impact of Carrier Transport and Capture on VCSEL Dynamics



Citation for the original published paper (version of record):
Grabowski, A., Gustavsson, J., Larsson, A. (2023). Impact of Carrier Transport and Capture on VCSEL Dynamics. IEEE Journal of Quantum Electronics, 59(1): 1-6.
http://dx.doi.org/10.1109/JQE.2023.3236396

This article has been accepted for publication in IEEE Journal of Quantum Electronics. This is the author's version which has not been fully edited and content may change prior to final publication. Citation information: DOI 10.1109/JQE.2023.3236396


# Impact of Carrier Transport and Capture on VCSEL Dynamics

Alexander Grabowski, *Member, IEEE*, Johan S. Gustavsson, and Anders Larsson, *Fellow, IEEE*

***Abstract*— Using a vertical-cavity surface-emitting laser (VCSEL) equivalent circuit model based on two carrier rate equations to include effects of carrier dynamics, we study the impact of carrier transport and capture on the small- and large-signal modulation response of high-speed VCSELs. The model also accounts for parasitics, current-induced self-heating, and gain compression. A variation of the effective capture time from 1 to 15 ps is found to have a large impact on the small-signal modulation response, with the 3 dB bandwidth decreasing from 40 to 15 GHz and the response transitioning from under-damped to over-damped. This is primarily due to the increasing low frequency parasitic-like roll-off with increasing effective capture time. A significant effect on the optical waveforms produced by the VCSEL under 56 Gbit/s on-off keying (OOK) non-return-to-zero (NRZ) and pulse-amplitude modulation 4 (PAM4) modulation is observed, with a short effective capture time leading to horizontal eye closure caused by timing jitter (TJ) and intersymbol interference (ISI) and a long effective capture time leading to vertical eye closure caused by long rise- and fall-times. However, for high modulation speed, a short effective capture time is needed and the photon lifetime should be set for clear eye opening. We also show the impact of the effective capture time on the output power vs current characteristics and map the dependence of internal temperature, carrier densities, carrier escape and leakage rates, and spontaneous recombination rates on current for different effective capture times.**

***Index Terms*— Semiconductor lasers, surface-emitting lasers, equivalent circuits, semiconductor device modeling, dynamic response, charge carrier lifetime, charge carrier density, charge carrier processes.**

## I. Introduction

CARRIER dynamics in the undoped region of the separate confinement heterostructure (SCH) and the quantum wells (QWs) is known to have an impact on the modulation response [1] and electrical impedance [2] of QW lasers. This includes vertical-cavity surface-emitting lasers (VCSELs) since all VCSELs employ QW active regions. However, to what extent carrier dynamics in these regions affects the small- and large-signal modulation response of VCSELs is not well known since it is difficult to control the parameters governing e.g. carrier transport in the SCH and carrier QW capture by design. This makes an experimental study virtually impossible.

Carrier transport and capture in the SCH and QWs is a complex process, including the relaxation of injected carriers within the band of unconfined states in the SCH region embedding the QWs, the diffusive carrier transport along the SCH, and the intrinsic capture of carriers into the confined states of the QWs [3]. The rate of this process is commonly quantified by a carrier effective capture time. Carrier transport along the SCH is mainly governed by diffusion [1], with the associated speed set by the diffusion coefficients. Relaxation of carriers to the ground state of the QWs occurs through LO phonon emission [3], carrier-carrier scattering [4], and impurity scattering [5]. Therefore, active region design parameters that are expected to impact VCSEL dynamics include e.g. the choice of materials and associated diffusion coefficients, the length of the SCH, and the energy spacing between QW subbands with respect to the LO phonon energy. Another important time constant is the carrier escape time from QWs which quantifies the rate at which carriers confined in the QWs are thermally excited back to the continuum of unconfined states in the SCH [6]. In addition, time constants related to spontaneous recombination in the SCH and the QWs [7], as well as leakage of carriers out of the SCH [8], are important for QW laser dynamics.

Carrier transport in SCH and capture in QWs has a direct impact on the small-signal modulation response of QW lasers [1]. The non-zero carrier effective capture time reduces the effective differential gain, which leads to reduced resonance frequency and enhanced damping. It also leads to a low frequency parasitic-like roll-off, which further reduces the bandwidth and enhances damping.

Here we use our physics-based equivalent circuit VCSEL model [9] to study the effects of carrier transport in SCH and QW capture on the VCSEL small- and large-signal modulation characteristics. The model is based on rate equations, with two rate equations for the carriers: one for the pool of unconfined carriers in the SCH and one for the pool of confined carriers in the QWs. Consequently, the effects of carrier dynamics in SCH and QWs are accounted for by the inclusion of all relevant time constants: carrier effective QW capture time ($\tau_{cap}$), carrier escape time from QWs ($\tau_{esc}$), carrier leakage time out of SCH ($\tau_{leak}$), and spontaneous recombination times in SCH and QW. The model also accounts for parasitic resistances and capacitances from the device layout and for the effects of

Manuscript received July 26, 2022; revised December 9, 2022. This work was supported by the Swedish Foundation for Strategic Research (SSF). (Corresponding author: Alexander Grabowski.)
Alexander Grabowski, Johan Gustavsson, and Anders Larsson are with the Photonics Laboratory, Department of Microtechnology and Nanoscience (MC2), Chalmers University of Technology, SE-41296 Gothenburg, Sweden (email: alexander.grabowski@chalmers.se; johan.gustavsson@chalmers.se; anders.larsson@chalmers.se).

This article has been accepted for publication in IEEE Journal of Quantum Electronics. This is the author's version which has not been fully edited and content may change prior to final publication. Citation information: DOI 10.1109/JQE.2023.3236396


current-induced device self-heating, and therefore provides more realistic data than models neglecting these effects.

## II. VCSEL AND EQUIVALENT CIRCUIT MODEL

The VCSEL under study is an 850 nm VCSEL with multiple strained InGaAs/AlGaAs QWs, a short optical cavity, and multiple oxide apertures for capacitance reduction [10]. With a 7 µm diameter primary oxide aperture and biased at 7.7 mA (the nominal bias current) for a current density of 20 kA/cm$^2$, the VCSEL exhibits a flat modulation response with a 3 dB bandwidth of 28 GHz at 25°C. In the following study, where we use the VCSEL equivalent circuit to quantify the impact of $\tau_{cap}$ on the VCSEL small- and large-signal modulation response, all simulations are done at an ambient temperature of 25°C.

The model, as mentioned earlier, accounts for the effects of carrier dynamics in the SCH and QWs, device electrical parasitics, and current-induced device self-heating, in addition to the intrinsic carrier-photon interaction in the QWs through stimulated emission with gain compression included. Several key VCSEL parameters are affected by the increasing internal device temperature with current. The model accounts for their temperature dependencies. This includes e.g. the resonance (lasing) wavelength, optical gain, spontaneous recombination parameters, internal optical loss (free carrier absorption), electrical resistances, and device thermal impedance, with temperature set by the ambient temperature and various self-heating effects [11], [12]. Escape of carriers from the QWs and leakage of carriers out of the SCH is treated using a thermionic emission model. Therefore, the escape and leakage times are strongly dependent on temperature and QW and SCH carrier densities, respectively. A detailed description of the model is presented in [9]. Contrary to the escape and leakage times, $\tau_{cap}$ is assumed temperature independent. This is an approximation, but is for the purpose of this study a fair assumption, since at the biasing point at which the large-signal simulations are done the differences in internal temperature between different $\tau_{cap}$ is small, meaning that the results are qualitatively valid.

A $\tau_{cap}$ of 7 ps was found to most accurately reproduce the measured DC, RF, and large-signal modulation characteristics [9]. We refer to this as the nominal carrier effective QW capture time. The intrinsic carrier QW capture time is expected to be around 1 ps at room temperature [3]. However, the intrinsic carrier QW capture time is enhanced by the ratio of the volume of the SCH and the total QW volume [1], which in our case is 3.7. The time representing diffusive transport along the SCH adds to this, rendering a $\tau_{cap}$ of 7 ps reasonable.

The rate equations used in the VCSEL model for the two carrier reservoirs and one photon reservoir are presented in [9], but are listed here for convenience:

$$\frac{dn_B}{dt} = i_{inj} - i_{sp,B} - i_{cap} + i_{esc} - i_{leak}, \quad (1)$$

$$\frac{dn_A}{dt} = i_{cap} - i_{sp,A} - i_{esc} - i_{st}, \quad (2)$$

$$\frac{dS}{dt} = i_{st} + i_{sp} - i_{abs} - i_{bm} - i_{tm}, \quad (3)$$

where $n_B$ is the number of carriers in the SCH, $n_A$ is the number of carriers in the QWs, and $S$ the number of photons in the resonator. The currents represent carrier and photon change rates [1/s], where $i_{inj}$ represents the carriers injected into the SCH, $i_{sp,B}$ the SCH spontaneous carrier recombination, $i_{cap}$ the capture of carriers into the QWs, $i_{esc}$ the escape of carrier out of the QWs, $i_{leak}$ the leakage of carriers out of the SCH, $i_{sp,A}$ the QW spontaneous carrier recombination, $i_{st}$ the QW stimulated emission, $i_{sp}$ the fraction of QW spontaneous emission that couples into the lasing mode, $i_{abs}$ the loss of photons through free-carrier absorption in the doped DBRs, and $i_{bm}$ and $i_{tm}$ the bottom and top DBR transmission losses, respectively.

The model does not account for any transverse spatial effects, and therefore assumes uniform bandgap and temperature profiles, as well as uniform current injection across the active area.

## III. SIMULATIONS

In the simulations, we have varied $\tau_{cap}$ from 1 to 15 ps to quantify the impact of carrier transport in SCH and capture in QWs on the modulation response under small-signal modulation and the optical waveforms generated by the VCSEL under 56 Gbit/s on-off keying (OOK) non-return-to-zero (NRZ) and pulse-amplitude modulation 4 (PAM4) large-signal modulation. DC simulations have also been performed to study the impact on the static characteristics.

The simulations were performed using the Cadence Spectre simulator, in a Cadence Virtuoso view implementation. We made use of a Verilog-A-implementation of the large-signal equivalent circuit VCSEL model presented in [9]. The input circuit for the simulations contains an effectively ideal bias-tee. Through this bias-tee, the VCSEL-model is biased with a current source and either driven with a pseudorandom binary sequence-7 (PRBS-7) voltage signal for the large-signal simulations or a standard port for the S-parameter simulations,

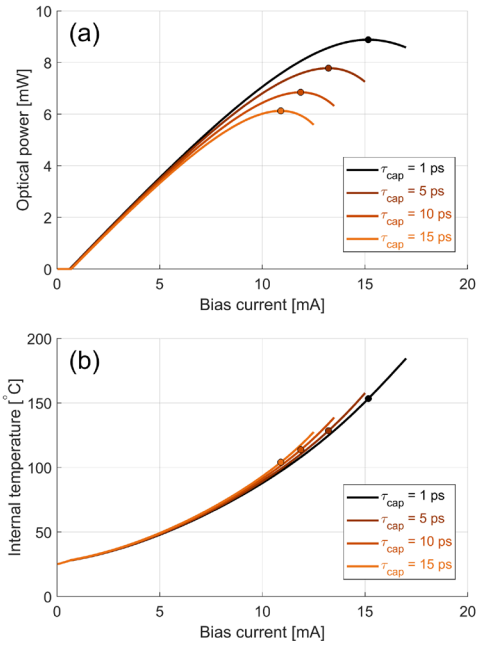


Fig. 1. Optical output power (a) and internal temperature (b) vs bias current, for different carrier effective QW capture times. Symbols indicate the rollover points.

This article has been accepted for publication in IEEE Journal of Quantum Electronics. This is the author's version which has not been fully edited and content may change prior to final publication. Citation information: DOI 10.1109/JQE.2023.3236396



both of which are disabled while performing the DC simulations.

In all figures, results are presented for a $\tau_{cap}$ of 1, 5, 10 and 15 ps. We have chosen these values because our nominal $\tau_{cap}$ is 7 ps, meaning that 15 ps should represent a relatively long carrier effective QW capture time using the VCSEL design and parameters described in [9]. As aforementioned, 1 ps is at room temperature an estimate of the intrinsic carrier QW capture time [3], suggesting that we cannot go lower even if limitations by carrier diffusion and relaxation were eliminated, thus making this our lower limit.

Fig. 1 (a) and (b), respectively, show the VCSEL optical output power and internal temperature as a function of bias current. From (a) it can be observed that a change of $\tau_{cap}$ does affect the power-current characteristics at high currents. The threshold current and the slope efficiency at low current are essentially unaffected while the maximum power and the associated rollover current are reduced with increasing $\tau_{cap}$. From (b) we observe stronger self-heating with longer $\tau_{cap}$ due to increased SCH spontaneous recombination and leakage rates, caused by a higher SCH carrier density (see next paragraph). In Figs. 1-3, the rollover points are indicated by symbols.

Fig. 2 (a) and (b), respectively, show the SCH and QW carrier density vs bias current. The QW carrier density at threshold is unaffected by variations of $\tau_{cap}$, which explains the constant threshold current (Fig. 1 (a)). With increasing current above threshold, there is a slow increase of the QW carrier density, although being clamped by stimulated emission. This is due to stronger gain compression with increasing photon density. On the other hand, the SCH carrier density, which is not clamped, increases rapidly with current above threshold at a rate that depends on $\tau_{cap}$. A shorter $\tau_{cap}$ will empty the SCH carrier reservoir at a faster rate, while a longer $\tau_{cap}$ will do this at a slower rate, hence leading to a faster increase of the SCH carrier density with current.

Fig. 3 (a)-(c), respectively, show the time constants for carriers escaping from the QWs ($\tau_{esc}$), carriers leaking out from the SCH ($\tau_{leak}$), and carriers spontaneously recombining in the QWs as a function of current. All time constants show the expected behavior, e.g. decreasing with current due to an increase of both QW and SCH carrier densities. We note that at the nominal bias current of 7.7 mA, $\tau_{esc}$ (≈ 55 ps) is about an order of magnitude higher than $\tau_{cap}$ and that the QW spontaneous recombination time (≈ 720 ps) is yet another order of magnitude higher. From Fig. 3 (b), we also note that rollover in output power occurs when $\tau_{leak}$ approaches 200 ps, independent of $\tau_{cap}$. This shows that rollover in output power is caused primarily by increasing carrier leakage from SCH with

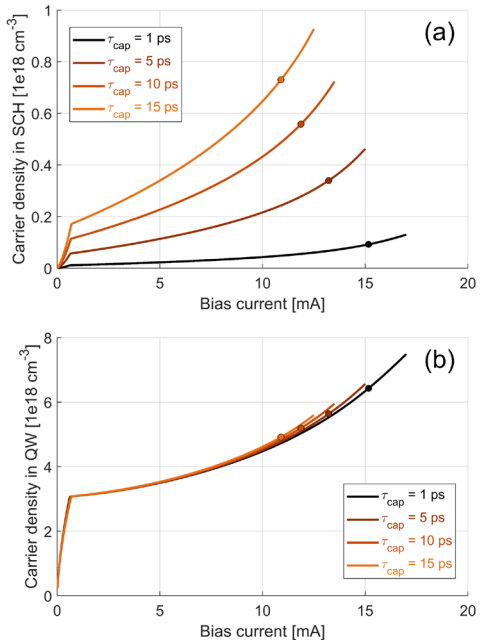


Fig. 2. Carrier density in SCH (a) and QW (b) vs bias current, for different carrier effective QW capture times. Symbols indicate the rollover points.

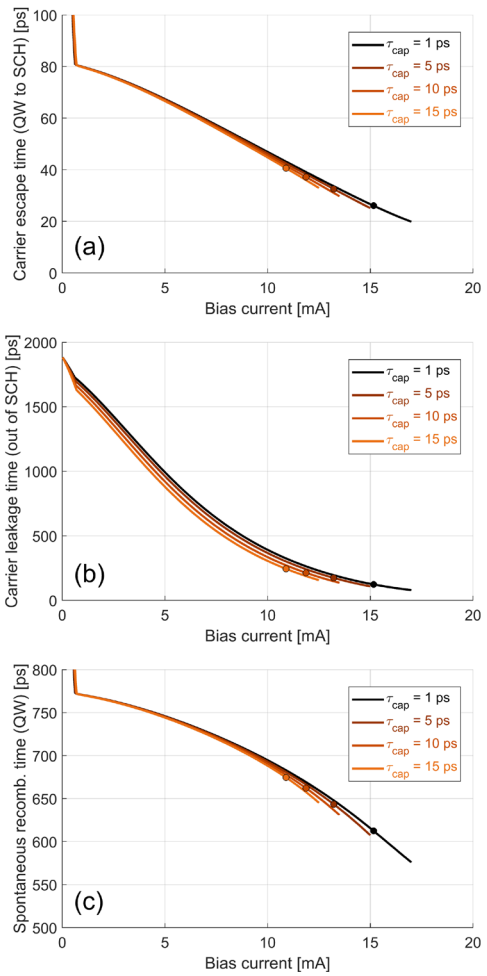


Fig. 3. Time constant for carrier escape from QWs (a), leakage out of SCH (b) and spontaneous recombination in QWs (c) vs bias current, for different carrier effective QW capture times. Symbols indicate the rollover points.

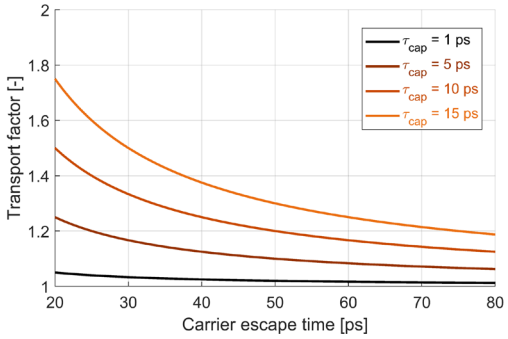


Fig. 4. Transport factor vs carrier escape time from QWs, for different carrier effective QW capture times.

increasing internal device temperature, in agreement with previous observations [8]. Because of the increasing SCH carrier density with increasing $\tau_{cap}$ (Fig. 2 (a)), rollover in output power occurs at a lower internal device temperature (Fig. 1). This is consistent with the thermionic emission model used for carrier leakage.

An important parameter introduced in [1] is the transport factor ($\chi$), which is defined as

$$\chi = 1 + \frac{\tau_{cap}}{\tau_{esc}}. \tag{4}$$

This parameter modifies the classical equations for the current dependence of the small-signal resonance frequency ($f_r$), damping rate ($\gamma$), and the associated $K$- and $D$-factors, according to [1],

$$f_r = D \cdot \sqrt{I - I_{th}}, \tag{5}$$

$$D = \frac{1}{2\pi} \cdot \sqrt{\frac{\eta_i \Gamma v_g}{qV_a} \cdot \frac{(\partial g/\partial \Delta n)}{\chi}}, \tag{6}$$

$$\gamma = K \cdot f_r^2 + \gamma_0, \tag{7}$$

$$K = 4\pi^2 \left(\tau_p + \frac{\varepsilon \cdot \chi}{v_g(\partial g/\partial \Delta n)}\right), \tag{8}$$

$$\gamma_0 = \frac{1}{\chi \tau_n}, \tag{9}$$

with all parameters defined in [1]. With $\chi$ being equal to or exceeding one (when $\tau_{esc}$ approaches $\tau_{cap}$), (6) and (8) show that the transport factor can reduce the effective differential gain, which leads to a reduced resonance frequency and an increased damping rate. Fig. 4 plots the transport factor according to (4). With $\tau_{esc} \approx 55$ ps at 7.7 mA, $\chi$ attains a maximum value of ~1.3 for $\tau_{cap}$ = 15 ps, which reduces the resonance frequency by about 10%. The impact on damping is expected to be less since, for high-speed VCSELs, the $K$-factor is typically dominated by the photon lifetime ($\tau_p$) [13].

Fig. 5 shows the VCSEL small-signal modulation response (magnitude of $S_{21}$) versus frequency at 7.7 mA bias current for the different $\tau_{cap}$. Consistent with the predictions regarding the resonance frequency, a ~10% reduction is observed when $\tau_{cap}$ is increased from 1 to 15 ps. However, with increasing $\tau_{cap}$, a more damped response than predicted by a reduction of the effective differential gain is observed. This is due to the enhanced low frequency parasitic-like roll-off with increasing

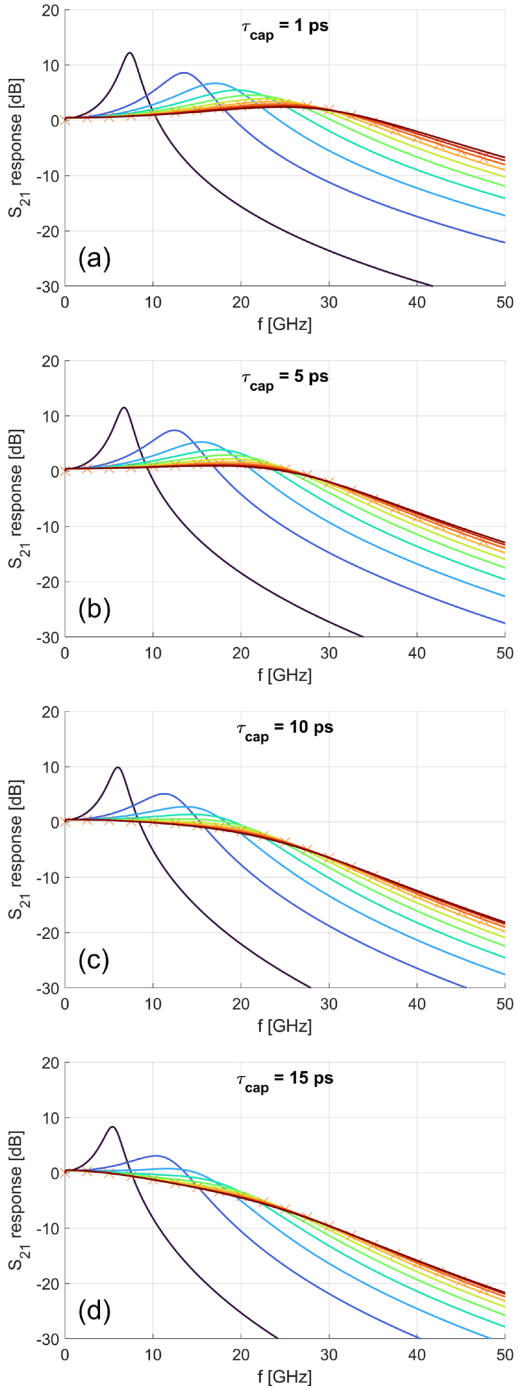


Fig. 5. Magnitude of $S_{21}$ response (normalized) vs frequency, for bias currents 1 to 10 mA in steps of 1 mA, with the 8 mA line clarified with cross symbols for comparison with the large-signal simulations, for carrier effective QW capture times 1 ps (a), 5 ps (b), 10 ps (c) and 15 ps (d).

$\tau_{cap}$. With $\tau_{cap}$ increasing from 1 to 15 ps, the 3 dB bandwidth is reduced from 40 to 15 GHz and the response transitions from being under-damped to critically damped and over-damped. This shows that $\tau_{cap}$ can indeed be a limiting factor for the modulation response and bandwidth of VCSELs and ultimately the maximum error-free data rate.

Fig. 6 shows the simulated large-signal modulation response (represented by eye diagrams) under OOK (NRZ) and PAM4 modulation with $\tau_{cap}$ varying from 1 to 15 ps. The peak-to-peak modulation voltage used is 380 and 900 mV for OOK and

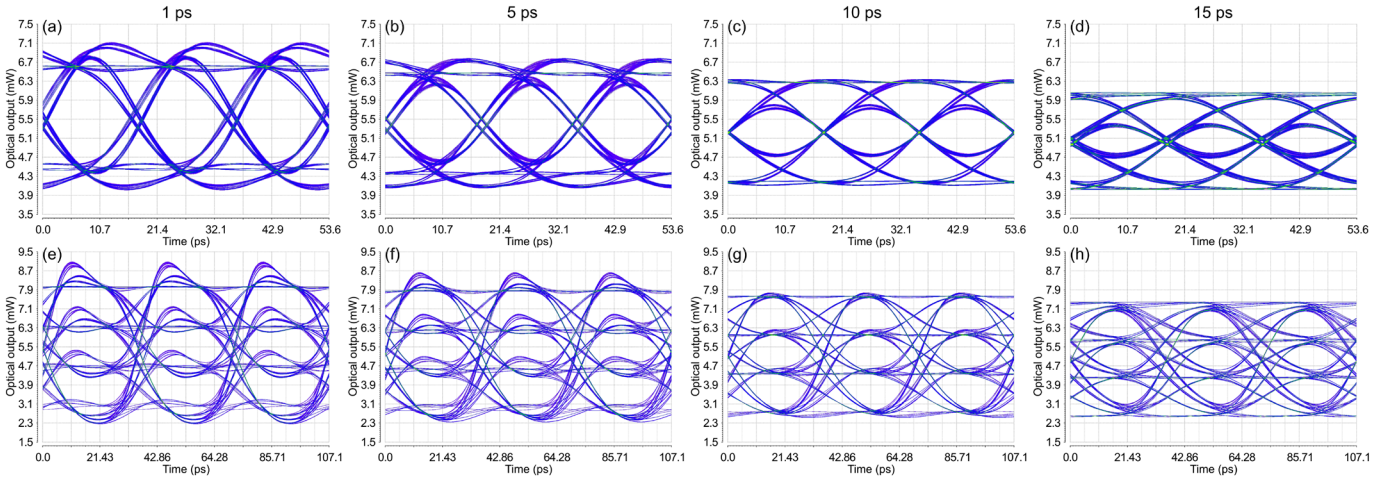


Fig. 6. Eye diagrams from large-signal simulations. The carrier effective QW capture time varies with column, from 1 to 15 ps, from left to right, and the two modulations formats are split between the rows, with OOK on the top row and PAM4 on the bottom. The VCSEL is biased at 7.7 mA.

PAM4, respectively. The VCSEL is biased at the nominal current of 7.7 mA. An analysis of the eye diagrams shows that the increased damping and reduced bandwidth with increasing $\tau_{cap}$ has a large impact on the quality of the optical waveforms, with increasing vertical eye closure due to longer rise- and fall-times. On the other hand, the under-damped response with a very short $\tau_{cap}$ results in excessive timing jitter (TJ) and intersymbol interference (ISI), leading to horizontal eye closure as clearly observed for the OOK modulation format. The effect is less pronounced for the PAM4 format due to the more complex multi-level transitions with inherently stronger ISI.

The effects observed when varying $\tau_{cap}$ are similar to those observed when varying the photon lifetime [14][15], with a short photon lifetime producing an under-damped response and a long photon lifetime producing a damped response. Therefore, for a given $\tau_{cap}$, the photon lifetime can adjusted for a flat and high bandwidth small-signal modulation response with clear eye opening under large-signal modulation at high data rates. This is most easily achieved by adjusting the reflectivity of the top-DBR [13]. A more damped response (by longer $\tau_{cap}$ or longer $\tau_p$) is generally beneficial for PAM4, as can be seen in Fig. 6 and in agreement with previous studies [15], since multi-level modulation formats are less immune to dynamic nonlinearities. In the model used [9], the value of $\tau_p$, determined by the rates at which photons are transmitted through the DBRs and lost by free-carrier absorption in the doped DBRs, is 3.9 ps at 7.7 mA, and hardly varies with $\tau_{cap}$.

The damping of the modulation response is also affected by parasitics and the current at which the VCSEL is biased. Larger resistances and capacitances lead to stronger low-pass filtering of the modulation current, which dampens the response and reduces the bandwidth. A more damped response can also be achieved by biasing at a higher current. However, a higher current may have a negative impact on reliability and for any VCSEL current should be limited to meet lifetime requirements.

Finally, we note the great uncertainty regarding the actual $\tau_{cap}$ for a given QW laser design under given operating conditions [1]. In our equivalent circuit model [9], the value of $\tau_{cap}$ that reproduces the measured DC, RF, and large-signal modulation behavior is to some extent affected by the choice of other parameters defining the circuit elements. Therefore, the results from this study should be used to gain insight into the general dependence of VCSEL performance on $\tau_{cap}$ and to highlight the importance of this parameter, rather than considering specific values of $\tau_{cap}$.

## IV. Conclusion

Since carrier transport in SCH and capture in QWs are known to affect the high-speed modulation behavior of QW lasers, including VCSELs, and since it is next to impossible to experimentally study the impact of $\tau_{cap}$ on VCSEL dynamics, we have examined these effects using our large-signal equivalent circuit VCSEL model.

The simulations confirm logical assumptions of a longer $\tau_{cap}$ reducing VCSEL bandwidth, primarily through an enhanced low frequency parasitic-like roll-off in the small-signal modulation response. With an increase of $\tau_{cap}$ from 1 to 15 ps, the small-signal modulation bandwidth is reduced from 40 to 15 GHz while the small-signal modulation response transitions from being under-damped to over-damped. This has a significant effect on the optical waveforms produced by the VCSEL under large-signal OOK and PAM4 modulation, with a short $\tau_{cap}$ leading to horizontal eye closure caused by TJ and ISI and a long $\tau_{cap}$ leading to vertical eye closure caused by long rise- and fall-times. On the other hand, to reach the highest possible modulation speed, a short $\tau_{cap}$ is needed and the photon lifetime should be set to balance the effects of $\tau_{cap}$ and $\tau_p$ for a high-bandwidth, critically damped response.

## Acknowledgment

This project was financially supported by the Swedish Foundation for Strategic Research (CHI19-0004).

## References

[1] R. Nagarajan, M. Ishikawa, T. Fukushima, R. S. Geels, and J. E. Bowers, "High speed quantum-well lasers and carrier transport effects," *IEEE J Quantum Electron*, vol. 28, no. 10, pp. 1990–2008, Oct. 1992, doi: 10.1109/3.159508.

[2] I. Esquivias, S. Weisser, B. Romero, J. D. Ralston, and J. Rosenzweig, "Carrier dynamics and microwave characteristics of

GaAs-based quantum-well lasers," *IEEE J Quantum Electron*, vol. 35, no. 4, pp. 635–646, Apr. 1999, doi: 10.1109/3.753669.

[3] R. Paiella, G. Hunziker, and K. J. Vahala, "Quantum-well capture and interwell transport in semiconductor active layers," *Semicond Sci Technol*, vol. 14, no. 5, pp. R17–R25, May 1999, doi: 10.1088/0268-1242/14/5/001.

[4] P. W. M. Blom, J. Claes, J. E. M. Haverkort, and J. H. Wolter, "Experimental and theoretical study of the carrier capture time," *Opt Quantum Electron*, vol. 26, no. 7, pp. S667–S677, Jul. 1994, doi: 10.1007/BF00326654.

[5] B. Deveaud, A. Chomette, D. Morris, and A. Regreny, "Carrier capture in quantum wells," *Solid State Commun*, vol. 85, no. 4, pp. 367–371, Jan. 1993, doi: 10.1016/0038-1098(93)90034-K.

[6] I. Esquivias *et al.*, "Carrier escape time in GaAs/AlGaAs and InGaAs/GaAs quantum well lasers," in *Proc. SPIE, High-Speed Semiconductor Laser Sources*, Apr. 1996, vol. 2684, pp. 17–26. doi: 10.1117/12.236950.

[7] G. E. Giudice, D. V. Kuksenkov, H. Temkin, and K. L. Lear, "Differential carrier lifetime in oxide-confined vertical cavity lasers obtained from electrical impedance measurements," *Appl Phys Lett*, vol. 74, no. 7, pp. 899–901, Feb. 1999, doi: 10.1063/1.123403.

[8] J. W. Scott, R. S. Geels, S. W. Corzine, and L. A. Coldren, "Modeling temperature effects and spatial hole burning to optimize vertical-cavity surface-emitting laser performance," *IEEE J Quantum Electron*, vol. 29, no. 5, pp. 1295–1308, May 1993, doi: 10.1109/3.236145.

[9] A. Grabowski, J. Gustavsson, Z. S. He, and A. Larsson, "Large-Signal Equivalent Circuit for Datacom VCSELs," *Journal of Lightwave Technology*, vol. 39, no. 10, pp. 3225–3236, May 2021, doi: 10.1109/JLT.2021.3064465.

[10] P. Westbergh, R. Safaisini, E. Haglund, J. S. Gustavsson, A. Larsson, and A. Joel, "High-speed 850 nm VCSELs with 28 GHz modulation bandwidth for short reach communication," in *Proc. SPIE, Vertical-Cavity Surface-Emitting Lasers XVII*, Mar. 2013, vol. 8639, pp. 86390X-1–6. doi: 10.1117/12.2001497.

[11] P. P. Baveja *et al.*, "Assessment of VCSEL thermal rollover mechanisms from measurements and empirical modeling," *Opt Express*, vol. 19, no. 16, p. 15490, Aug. 2011, doi: 10.1364/OE.19.015490.

[12] P. P. Baveja *et al.*, "Impact of Device Parameters on Thermal Performance of High-Speed Oxide-Confined 850-nm VCSELs," *IEEE J Quantum Electron*, vol. 48, no. 1, pp. 17–26, Jan. 2012, doi: 10.1109/JQE.2011.2176554.

[13] P. Westbergh, J. S. Gustavsson, B. Kögel, A. Haglund, and A. Larsson, "Impact of Photon Lifetime on High-Speed VCSEL Performance," *IEEE Journal of Selected Topics in Quantum Electronics*, vol. 17, no. 6, pp. 1603–1613, Nov. 2011, doi: 10.1109/JSTQE.2011.2114642.

[14] E. P. Haglund, P. Westbergh, J. S. Gustavsson, and A. Larsson, "Impact of Damping on High-Speed Large Signal VCSEL Dynamics," *Journal of Lightwave Technology*, vol. 33, no. 4, pp. 795–801, Feb. 2015, doi: 10.1109/JLT.2014.2364455.

[15] T. Lengyel *et al.*, "Impact of Damping on 50 Gbps 4-PAM Modulation of 25G Class VCSELs," *Journal of Lightwave Technology*, vol. 35, no. 19, pp. 4203–4209, Oct. 2017, doi: 10.1109/JLT.2017.2727549.

**Alexander Grabowski** received his M.Sc. degree in electrical engineering and his Ph.D. degree from Chalmers University of Technology, Göteborg, Sweden, in 2017 and 2022, respectively. He is currently working as a postdoc at the Department of Microtechnology and Nanoscience at Chalmers. He is working on GaAs-based vertical-cavity surface-emitting lasers (VCSELs) in high-speed short-reach optical interconnects, mainly focusing on modelling of the VCSEL. He has also done work on fabrication of GaAs-based VCSELs for micro-transfer-printing integration on a silicon nitride PIC platform.

**Johan S. Gustavsson** received his M.Sc. degree in Electrical Engineering and his Ph.D. degree in Photonics from Chalmers University of Technology, Göteborg, Sweden, in 1998 and 2003, respectively. His Ph.D. thesis was focused on mode dynamics and noise in vertical-cavity surface-emitting lasers (VCSELs). Since 2003 he has been a researcher at the Photonics Laboratory, at Chalmers, with an Assistant Professor position 2004-2008, and an Associate Professor position from 2011. In Sept.-Oct. 2009 he was a visiting scientist at CNR Polytechnico, Turin, Italy, and in 2017 he co-organized the European Semiconductor Laser Workshop in Copenhagen. In 2016, he co-founded the spin-off company OptiGOT AB, which was in 2020 acquired by Nvidia Corp. He has authored or coauthored more than 250 scientific journal and conference papers and two book chapters, and his research has been focused on semiconductor lasers for short to medium reach communication, and sensing applications. This has included surface relief techniques for mode and polarization control in VCSELs, 1.3 µm InGaAs VCSELs/GaInNAs ridge waveguide lasers for access networks, 2.3-3.5 µm GaSb VCSELs for CO, $CO_2$ and $NH_3$ sensing, and tunable VCSELs via moveable mirror for reconfigurable optical interconnects. He is currently working on energy efficient 56 Gbaud GaAs-based VCSELs for next generation datacom links, UV/blue AlGaN/GaN VCSELs for sterilizing/illumination, high contrast gratings as feedback/wavelength setting/focusing elements in micro-cavity lasers, and heterogeneous integration of III/V-based VCSEL material on a Si-platform. He is also exploring photon-photon resonance effects to boost the modulation bandwidth in GaAs-based VCSELs.

**Anders Larsson** received the M.Sc. and Ph.D. degrees in electrical engineering from Chalmers University of Technology, Göteborg, Sweden, in 1982 and 1987, respectively. In 1991, he joined the faculty at Chalmers where he was promoted to Professor in 1994. From 1984 to 1985, he was with the Department of Applied Physics, California Institute of Technology, and from 1988 to 1991 with the Jet Propulsion Laboratory, both at Pasadena, CA, USA. He has been a guest professor at Ulm University (Germany), at the Optical Science Center, University of Arizona at Tucson (USA), at Osaka University (Japan), and at the Institute of Semiconductors, Chinese Academy of Sciences (China). He co-organized the IEEE Semiconductor Laser Workshop 2004, organized the European Semiconductor Laser Workshop 2004, was a co-program chair for the European Conference on Optical Communication 2004, and was the program and general chair for the IEEE International Semiconductor Laser Conference in 2006 and 2008, respectively. He was a member of the IEEE Photonics Society Board of Governors (2014-2016), an associate editor for IEEE/OSA Journal of Lightwave Technology (2011-2016) and a member of the editorial board of IET Optoelectronics (2007-2020). In 2016, he co-founded OptiGOT AB, which was acquired by Nvidia in 2020. His scientific background is in the areas of optoelectronic materials and devices for optical communication, information processing, and sensing. Currently, his research is focused on vertical-cavity surface-emitting lasers and optical interconnects. He has published close to 600 scientific journal and conference papers and 2 book chapters. He is a Fellow of IEEE, OSA, and EOS. In 2012, he received the HP Labs Research Innovation Award.